International Journal of Heat and Mass Transfer 101 (2016) 981–987

Contents lists available at ScienceDirect

International Journal of Heat and Mass Transfer

journal homepage: www.elsevier.com/locate/ijhmt

Multi-objective genetic optimization of the heat transfer for tube inserted with porous media

Ya Ge, Zhichun Liu *, Wei Liu

School of Energy and Power Engineering, Huazhong University of Science and Technology, Wuhan 430074, PR China

ARTICLE INFO

Article history:
Received 5 April 2016
Received in revised form 12 May 2016
Accepted 27 May 2016
Available online 10 June 2016

Keywords:
Heat transfer enhancement
Porous media
Multi-objective optimization
Genetic algorithm
TOPSIS

ABSTRACT

This work is aimed at determining the best configurations of porous media inserted in a tube to achieve the excellent performance of fluid flow and heat transfer. Both geometry parameters and property parameters are the variables to be optimized. In order to evaluate the performance of tube, two conflicting objectives, Nusselt number *Nu* and friction factor *f*, are simultaneously considered. In the optimization process, computational fluid dynamics (CFD) and multi-objective genetic algorithm are coupled to obtain the numerical solutions of two-dimensional calculation model and Pareto front composed of non-inferior solutions. Besides, an attempt of utilizing limited resources is made by applying the penalty function instead of adding or modifying governing equations to restrain the flow resistance. Subsequently, technique for order preference by similarity to an ideal solution (TOPSIS) is employed to help decision makers determine the best alternative from the Pareto front. The results selected by TOPSIS are compared with the alternative which has the maximum Nusselt number. It is found that TOPSIS is effective to balance deferent objectives and determine compromise parameters.

1. Introduction

With the development of modern industry, the performance of heat exchangers becomes more and more important. In recent decades, considerable studies of heat transfer enhancement technologies and theories by disturbing fluid or increasing heat transfer area [1–3] in tubes have been made to meet the requirements of the energy saving. Recently, performances of tube with porous inserts have received some attention with experimental, analytical and numerical studies [4–7]. Mohamad [4] investigated heat transfer enhancement for a flow in a pipe or a channel fully or partially filled with porous media and found that partially filling has a better performance on both heat transfer and pressure drop. Huang et al. [5] studied the heat transfer enhancement for the flow in a pipe filled with annular porous ring and found that high porosity was recommended when using performance evaluation criteria (*PEC*) [6] as decision criteria. Zheng et al. [7] applied genetic algorithm (GA) to optimize the configurations of porous media which was divided into several layers and partially inserted in a tube. It was found that multiple layers of porous inserts can further increase the *PEC*.

When optimizing a heat transfer unit or a system, the flow resistance often has an increase with the enhancement of heat transfer. Therefore, evaluation criteria play a significant role in assessing the performance or determining the economic benefit of heat exchangers for many practical applications, such as *PEC*, *JF* factor [8], efficiency evaluation criterion (*EEC*) [9]. In existing studies, most of the evaluation criteria are composed of several parameters affecting the heat transfer and pressure-drop in a certain form. However, it is sometimes difficult to establish a general selection criterion to be applied in the industry. Recently, more and more optimizations attempt to apply multi-objective optimization techniques to obtain the non-inferior solutions, and choose the most feasible solution to meet the requirements for practical applications. This approach has been proven effective, and extensively applied in optimization design of different fields, such as thermodynamic cycle [10], power system [11].

In spite of the widespread application of multi-objective optimization techniques, there is limited published literature about optimizing the performance of tube with porous ring inserted. The purpose of this paper is to determine the optimal parameters of the porous media by means of a multi-objective genetic algorithm (MOGA) [12]. The geometrical shape and property configuration of porous ring jointly decide the performance of tube. Meanwhile, two conflicting objectives, Nusselt number *Nu* and friction factor *f*, are considered to be optimized at the same time. In

* Corresponding author.
E-mail address: zcliu@hust.edu.cn (Z. Liu).

http://dx.doi.org/10.1016/j.ijheatmasstransfer.2016.05.118
0017-9310/

Nomenclature

C	relative closeness to the ideal solution
c	specific heat
Da	Darcy number, K/r_0^2
F	inertia coefficient
H	convective heat transfer coefficient
f	friction factor
J	objective function
K	permeability
L_1	dimensionless entrance length
L_2	dimensionless exit section length
Nu	local Nusselt number, $2hr_0/\lambda_f$
P	dimensionless pressure
p	pressure
Pr	Prandtl number of the fluid, $c\mu_f/\lambda_f$
q	heat flux
R	dimensionless radius
R_1	dimensionless distance between the internal wall of porous ring and the centerline
R_2	dimensionless distance between the exterior wall of porous ring and the centerline
r	radial position measured from the centerline
r_0	radius of the tube
Re	Reynolds number, $2\rho ur_0/\mu_f$
T	temperature
U	dimensionless axial velocity
u	axial velocity
V	dimensionless radial velocity
v	radial velocity
X	dimensionless axial coordinate
x	axial position measured from the inlet

Greek symbols

ε	porosity
θ	dimensionless temperature
λ	thermal conductivity
μ	dynamic viscosity
ρ	fluid density

Superscript

e	effective
f	fluid domain properties
p	porous domain properties
R	the ratio of a parameter in porous domain to the same parameter in fluid domain
m	mean
s	solid matrix propertied
w	wall

present study, an effective design method [13] coupling GA and computational fluid dynamics (CFD) analyzes is applied to solve the multi-objective problems mentioned above. Subsequently, all the non-inferior solutions (Pareto solutions) obtained by MOGA are ranked by a famous decision making technique, TOPSIS (technique for order preference by similarity to an ideal solution) [14]. Besides, an attempt is made to restrain the flow resistance by employing the penalty function instead of adding or modifying governing equations.

2. Problem description and constraint conditions

2.1. Physical model

The schematic of the tubes inserted with porous ring in current study is shown in Fig. 1. A two-dimensional, centrosymmetric numerical model for convection heat transfer of steady laminar flow in a tube with constant heat flux is considered. In order to give function boundary conditions at the inlet and eliminate the influence of backflow at the outlet, an entrance section and an exit section are applied, respectively. The total length L is fixed at 24, with the entrance length $L_1 = 1$ and exit section length $L_2 = 3$. At the end of entrance section, a porous ring is placed in porous section with its length $L_p = 20$. As shown the Fig. 1, the position of porous ring can be determined by two parameters, R_1 and R_2. To simplify the analysis, other assumptions are listed as follows: (1) the porous media is regarded as homogeneous and isotropic; (2) the heat generated by the viscous effects is negligible; (3) the gravitational effect of the air flowing through the tube is negligible; (4) the gas phase and the solid phase in porous media exist in a state of local thermal equilibrium.

2.2. Mathematical model

The governing equations including the continuity, momentum, and energy can be expressed as follows [15]:

Continuity equation:

$$\frac{\partial(\rho u)}{\partial x}+\frac{1}{r}\frac{\partial(r\rho v)}{\partial r}=0 \tag{1}$$

Momentum in x-direction:

$$\begin{aligned}&\frac{\partial}{\partial x}\left(\frac{\rho}{\varepsilon}uu\right)+\frac{1}{r}\frac{\partial}{\partial r}\left(r\frac{\rho}{\varepsilon}vu\right)\\&=-\frac{\partial p}{\partial x}+\frac{\partial}{\partial x}\left(\frac{\mu}{\varepsilon}\frac{\partial u}{\partial x}\right)+\frac{1}{r}\frac{\partial}{\partial r}\left(r\frac{\mu}{\varepsilon}\frac{\partial u}{\partial r}\right)-\delta\frac{\mu_e u}{K}-\delta\frac{\rho F\varepsilon}{\sqrt{K}}|u|u\end{aligned} \tag{2}$$

Momentum in r-direction:

$$\begin{aligned}&\frac{\partial}{\partial x}\left(\frac{\rho}{\varepsilon}uv\right)+\frac{1}{r}\frac{\partial}{\partial r}\left(r\frac{\rho}{\varepsilon}vv\right)\\&=-\frac{\partial p}{\partial r}+\frac{\partial}{\partial x}\left(\frac{\mu}{\varepsilon}\frac{\partial v}{\partial x}\right)+\frac{1}{r}\frac{\partial}{\partial r}\left(r\frac{\mu}{\varepsilon}\frac{\partial v}{\partial r}\right)-\delta\frac{\mu_e v}{K}-\delta\frac{\rho F\varepsilon}{\sqrt{K}}|u|v-\frac{\mu v}{\varepsilon r^2}\end{aligned} \tag{3}$$

where ε is the porosity and K is the permeability. In this study, the parameter δ is set to unity for flow in porous medium and to zero for flow in a clear region. The inertia coefficient F is related to porosity as described by Ergun [16]:

$$F=\frac{1.75}{\sqrt{150\varepsilon^3}} \tag{4}$$

Energy equation:

$$\begin{aligned}&\frac{\partial}{\partial x}(\rho cuT)+\frac{1}{r}\frac{\partial}{\partial r}(\rho crvT)\\&=\frac{\partial}{\partial x}\left\{[\delta(\lambda_e-\lambda)+\lambda]\frac{\partial T}{\partial x}\right\}+\frac{1}{r}\frac{\partial}{\partial r}\left\{r[\delta(\lambda_e-\lambda)+\lambda]\frac{\partial T}{\partial r}\right\}\end{aligned} \tag{5}$$

where λ_e is the effective thermal conductivity of the porous media, $\lambda_e=\varepsilon\lambda_f+(1-\varepsilon)\lambda_s$ [17].

The boundary conditions are used as follows:

(1) at $r = 0$: $\frac{\partial u}{\partial r}=0,\ v=0,\ \frac{\partial T}{\partial r}=0$;
(2) at $r = r_0$: $u=0,\ v=0,\ \frac{\partial T}{\partial r}=-\frac{q}{\lambda_f}$;
(3) at $x = 0$: $u(r)=u_c\left[1-\left(\frac{r}{r_0}\right)^2\right],\quad v=0,\quad T(r)=T_c+\frac{qr_0}{\lambda_f}\left[\left(\frac{r}{r_0}\right)^2-\frac{1}{4}\left(\frac{r}{r_0}\right)^4\right]$;
(4) at $x = 24r_0$: $\frac{\partial u}{\partial x}=0,\ v=0,\ \frac{\partial T}{\partial x}=0,\ p=0$.

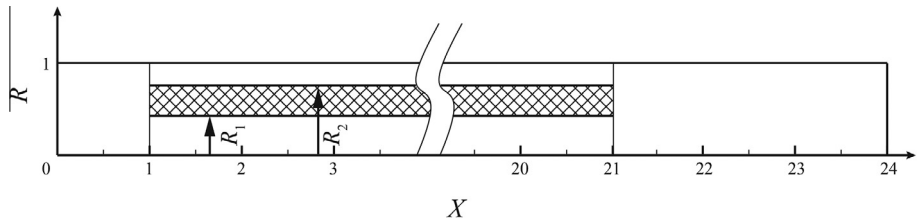

Fig. 1. Schematic diagram of the problem under consideration.

The above Eqs. (1)–(3) and (5) can be transformed into dimensionless forms by using dimensionless parameters:

$$Da = \frac{K}{r_0^2};\ U = \frac{u}{u_{in}};\ V = \frac{v}{u_{in}};\ P = \frac{p}{\rho u_{in}^2};\ \theta = \frac{T - T_{in}}{qr_0/\lambda};\ R = \frac{r}{r_0};\ X = \frac{x}{r_0} \tag{6}$$

The dimensionless set of equations is as follows:

$$\frac{\partial}{\partial X}(UU) + \frac{1}{R}\frac{\partial}{\partial R}(RVU) = -\frac{\partial P}{\partial X} + \frac{\partial}{\partial X}\left(\frac{\partial U}{\partial X}\right) + \frac{1}{R}\frac{\partial}{\partial R}\left(R\frac{\partial U}{\partial R}\right) - \delta\frac{U}{ReDa} - \delta\frac{F}{\sqrt{Da}}|U|U \tag{7}$$

$$\frac{\partial}{\partial X}(UV) + \frac{1}{R}\frac{\partial}{\partial R}(RVV) = -\frac{\partial P}{\partial R} + \frac{\partial}{\partial Z}\left(\frac{\partial V}{\partial Z}\right) + \frac{1}{R}\frac{\partial}{\partial R}\left(R\frac{\partial V}{\partial R}\right) - \delta\frac{V}{ReDa} - \delta\frac{F}{\sqrt{Da}}|U|V - \frac{V}{ReR^2} \tag{8}$$

$$\frac{\partial}{\partial X}(U\theta) + \frac{1}{R}\frac{\partial}{\partial R}(RV\theta) = \frac{1}{RePr}\left[\frac{\partial^2\theta}{\partial X^2} + \frac{1}{R}\frac{\partial}{\partial R}\left(R\frac{\partial\theta}{\partial R}\right)\right] \tag{9}$$

In this study, the Reynolds number is fixed at 100 and the Prandtl number of flow is fixed at 0.7. The above governing equations along with the boundary conditions are solved by adopting the finite-element method. In each case of the simulation, the flow and thermal field are computed with approximately 12,000 elements and 100,000 degrees of freedom. Furthermore, the direct problem is solved by commercial software COMSOL Multiphysics in this paper and it takes about 15–20 s to obtain one fitness value for a single individual when a personal computer with an Intel Xeon E3-1230 v2 CPU is used for computing.

3. Optimization method

3.1. Optimization functions

In this paper, two objective functions are defined as follows:

$$J_1 = f,\ J_2 = -Nu_{average} \tag{10}$$

as mentioned above, Nusselt number Nu is calculated to appraise the performance of heat transfer, while friction factor f is calculated to appraise the performance of flow resistance, respectively. The friction factor can be calculated from:

$$f = \frac{\Delta p}{l}\frac{2r_0}{(1/2)\rho u^2} \tag{11}$$

on the other hand, the local Nusselt number can be calculated from:

$$Nu(x) = \frac{2h(x)r_0}{\lambda_f} \tag{12}$$

one can obtain the value for local convective heat transfer coefficient $h(x)$ from:

$$h(x) = \frac{q}{T_w(x) - T_m(x)} \tag{13}$$

where $T_w(x)$ is the local temperature measured on the heated wall. The local mean thermodynamic temperature $T_m(x)$ can be calculated from:

$$T_m(x) = \frac{\int_0^{r_0} uTrdr}{\int_0^{r_0} urdr} \tag{14}$$

Therefore, as the objective function J_1 and J_2 are approaching minimum values in iterative process, an optimal tube with low flow resistance and high heat transfer coefficient can be achieved.

3.2. Design parameters

The goal is to find the optimal parameter configurations of the porous ring that maximizes heat transfer and minimizes flow resistance in the tube simultaneously. Therefore, all factors that affect the flow field structure and heat exchange capability should be taken into consider. In present study, R_1, R_2, ε and Da are defined as four variables which will be optimized by GA.

3.3. Multi-objective genetic algorithm

For many complex engineering problems, objectives under consideration often conflict with each other. When optimizing heat transfer units or systems, there is a common phenomenon that several objective functions are combined into a single composite objective function for evaluating the overall performance, such as utility theory, weighted sum method. The multi-objective evolutionary algorithms (MOEAs), however, are generalized approaches to determine an entire Pareto optimal solution set. In the present study, an efficient MOEA, the non-dominated sorting genetic algorithm (NSGA-II) [12], is employed to optimize two objective functions defined above. Following the concept of this algorithm, all individuals are ranked according to their fitness score based on the objective function values. Subsequently, in the process of producing the next generation, the individuals with high fitness score are more likely to be selected and preserved. Therefore, as the iterative process continues, the Pareto optimal solutions will be evolved gradually by the algorithm.

3.4. Optimization procedure

In this paper, the direct heat transfer problem described in Section 3.1 is solved by finite element software Comsol Multiphysics, and the validity of results will be discussed in further section. After calculating two objective functions J_1 and J_2 by Comsol, another commercial software Matlab [18] is used to process the data and apply multi-objective genetic algorithm. The related files with algorithm code are included in the genetic algorithm and direct searching toolbox (GADST). It is worth noting that coupling Comsol and Matlab is convenient for users because the communication and call methods between these two softwares do not require complex manual configurations. Meanwhile, this coupling method has been proved effective for optimizing heat transfer unit in our previous work [13]. By this method, a group of Pareto solutions are obtained according to the initial parameters. It takes about 50 h to finish one optimization process and the whole procedure is shown in Fig. 2.

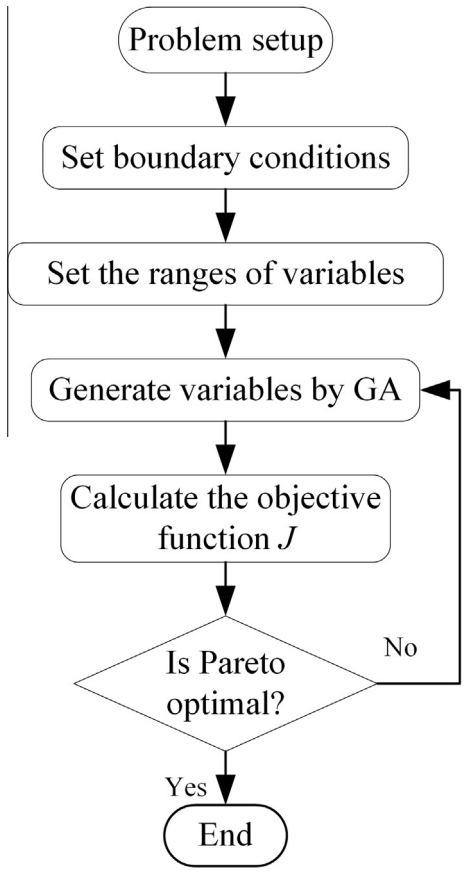

Fig. 2. Flow chart of the optimization process by GA.

3.5. TOPSIS selection

After deriving the Pareto front, the next step is to determine the best compromise solution for application. In general, selection work in multi-objective optimization is more complex since each Pareto solution represents a compromise solution under different objective functions and we cannot directly choose the best one. However, following the basic concept that the chosen alternative should have the shortest distance from the positive ideal solution and the longest distance from the negative ideal solution, TOPSIS is a practical and classical approach for ranking and selecting alternatives. The selection procedure of TOPSIS is as follows:

(1) Create a matrix $(x_{ij})_{m\times n}$ with m alternatives and n objectives.
(2) Normalize the matrix $(x_{ij})_{m\times n}$ to $(t_{ij})_{m\times n}$ by using the equation below:

$$t_{ij} = \frac{x_{ij}}{\sqrt{\sum_{i=1}^{m} x_{ij}^2}},\ i = 1,2,...,m,\ j = 1,2,...,n \tag{15}$$

(3) Obtain the weighted normalized matrix $(a_{ij})_{m\times n}$ by:

$$a_{ij} = w_j \times t_{ij}, i = 1,2,...,m,\ j = 1,2,...,n \tag{16}$$

(4) Determine the positive ideal alternative A^+ and the negative ideal alternative A^-:

$$A^+ = (\min[a_{11},...a_{m1}], \min[a_{12},...a_{m2}],...,\min[a_{1n},...a_{mn}]) \tag{17}$$

$$A^- = (\max[a_{11},...a_{m1}], \max[a_{12},...a_{m2}],...,\max[a_{1n},...a_{mn}]) \tag{18}$$

(5) Calculate the distance between the target alternative A and the positive ideal alternative A^+, and the distance between the target alternative A and the negative ideal alternative A^-:

$$d_i^+ = \sqrt{\sum_{j=1}^{n}(a_{ij} - A_j^+)^2},\ i = 1,2,...,m,\ j = 1,2,...,n \tag{19}$$

$$d_i^- = \sqrt{\sum_{j=1}^{n}(a_{ij} - A_j^-)^2},\ i = 1,2,...,m,\ j = 1,2,...,n \tag{20}$$

(6) Calculate the relative closeness to the ideal solution of alternatives:

$$C_i = \frac{d_i^-}{d_i^+ + d_i^-},\ i = 1,2,...,m \tag{21}$$

(7) Rank the alternatives according to the values of C_i, and the final compromise solution A_{final} is

$$A_{\text{final}} = A \in \max(C_i) \tag{22}$$

4. Results and discussion

4.1. Validation

In order to check the validity of present direct problem solver, Figs. 3 and 4 are plotted. Fig. 3 shows comparison between the present fully developed axial velocity profile and the previous one presented by Pavel and Mohamad [4]. Both Darcy–Brinkman–Forchheimer (DBF) model [19] and Darcy–Brinkman (DB) model [20] are compared with the previous work (DB model). It is found that velocity profile is basically identical to the previous one when DB model is applied in present work. Compared with DB model, the inertia coefficient F is unequal to zero in DBF model. As a result, the increased porous resistance forces more fluid to escape to the clear region. On the other hand, variation of the average Nusselt number with the different thickness of the porous substrate is plotted in Fig. 4. The result also shows that the maximum difference of Nusselt number between the present work and the previous one is 4.47%. Besides, the grid independence is checked when porous ring (for $Da = 10^{-3}$, $\varepsilon = 0.9$, $R_1 = 0.2$ and $R_2 = 0.8$) is inserted. Meshes in different sizes of 48,216, 96,580, and 253,800 are tested and the values of Nu are 14.943, 14.903, and 14.904 respectively. Therefore, the cases with the second mesh in this work are accurate enough to be applied in the next optimization procedure.

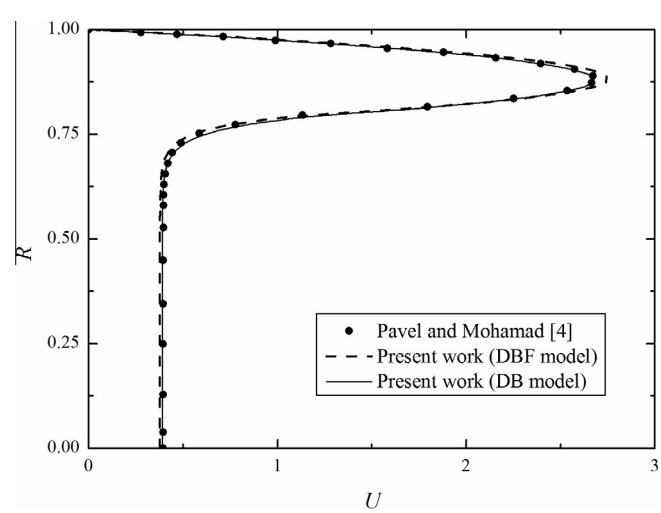

Fig. 3. Comparision of present fully developed velocity profile, U, with previous work obtained by Pavel and Mohamad [4], for $Da = 10^{-3}$, $R_1 = 0$ and $R_2 = 0.8$.

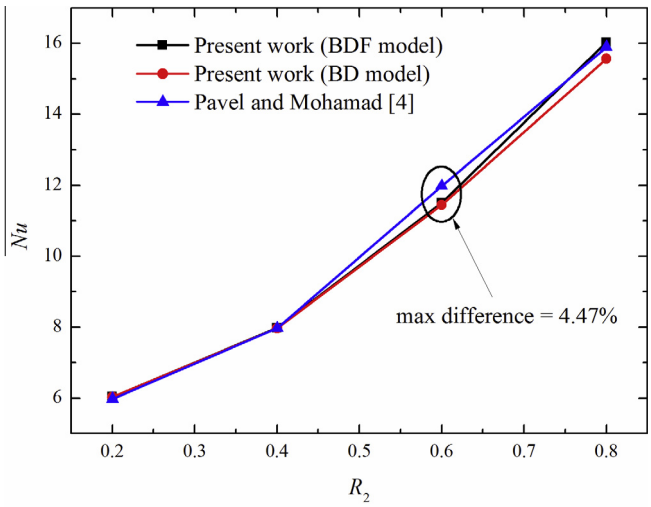

Fig. 4. Comparision of present fully developed Nusselt number, *Nu*, with previous work obtained by Pavel and Mohamad [4], for $Da = 10^{-3}$ and $R_1 = 0$.

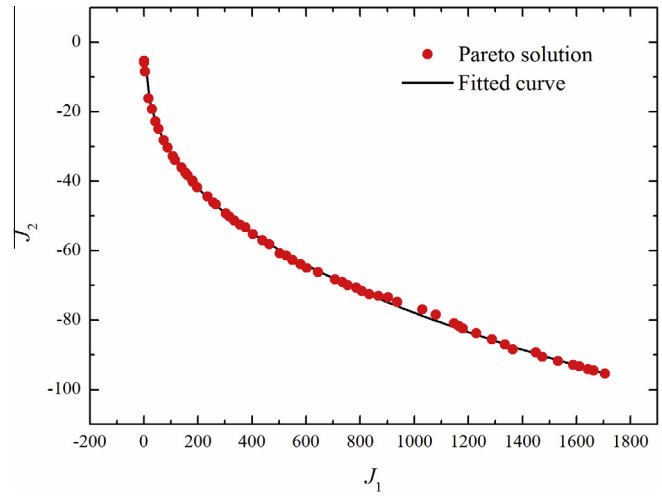

Fig. 5. Pareto solutions and fitted curve for the tube with porous insert.

4.2. Optimal results

The present results have been computed by using the following design parameters:

$$\lambda_R = 100,\ \mu_R = 1,\ \rho_R = 1,\ c_R = 1 \tag{23}$$

Besides, the geometrical variables and property variables for the optimization of the present configurations are allowed to vary with the following ranges:

$$\begin{aligned} &0.05 < R_1 < R_2 < 0.95 \\ &0.8 < \varepsilon < 0.98 \\ &10^{-8} < Da < 10^{-2} \end{aligned} \tag{24}$$

To ensure successful mesh generation, gap width between the porous media and wall (or centerline) is at least 0.05. The configurations of property variables refer to some familiar porous media. The multi-objective optimization problem with constrains mentioned above is solved by coupling Matlab and Comsol Multiphysics. The detailed configurations of genetic algorithm are listed in Table. 1.

The Pareto front containing 60 non-inferior solutions is illustrated in Fig. 5. For the same velocity inlet boundary condition, porous media with different parameters have significant impact on the performance of tube. It is found that the Nusselt number *Nu* varies from 5.28 to 95.36 and the friction factor *f* varies from 1.14 to 1705.2, which are enormously different from the clear tube ($Nu = 4.36$, $f = 0.64$). In order to investigate the functional relationship between J_1 and J_2, a power function is adopted to fit the curve. The fitted curve can be described by:

$$y(x) = -5.902x^{0.3752} + 1.177 \tag{25}$$

Fitting results shows that both the *R*-square (coefficient of determination) and the adjusted *R*-square (degree-of-freedom adjusted coefficient of determination) are 0.9995, which means the power function used above is accurate enough to describe the functional relationship between J_1 and J_2. The structure of equation shows that the further increase for *Nu* will be much more difficult than early stages because the growth rate of flow resistance is much higher. However, such a high flow resistance system is sometimes too difficult for the pumps to drive the fluid flow. Therefore, it is meaningful to investigate the detailed optimal solutions when *f* is not too high for the system.

In general, it is difficult to impose constraints by adding or modifying governing equations of flow field. In present study, however, utilizing the penalty function which is based on the concept of genetic algorithm makes this process much simpler. A penalty method replaces a constrained optimization problem by a series of unconstrained problems. By this method, infeasible solutions are allowed into the population but the fitness values are modified according to the penalty function. After sufficient time, the optimal solutions to the unconstrained problem using the modified fitness values coincide with the optimal solutions to the original constrained problem [21]. To be specific, we assigned $J_2 = 0$ to the individuals with $f > 50$ in the process of calculating individual fitness, so that those individuals would be eliminated gradually as a result of competition mechanism. Fig. 6 shows the Pareto front under the constraint of $f < 50$. The fitted curve can be described by:

Table 1
Operating parameters of the genetic algorithm.

Population of individuals	100
Generations	100
Elite count	2
Crossover fraction	0.8
Pareto fraction	0.6

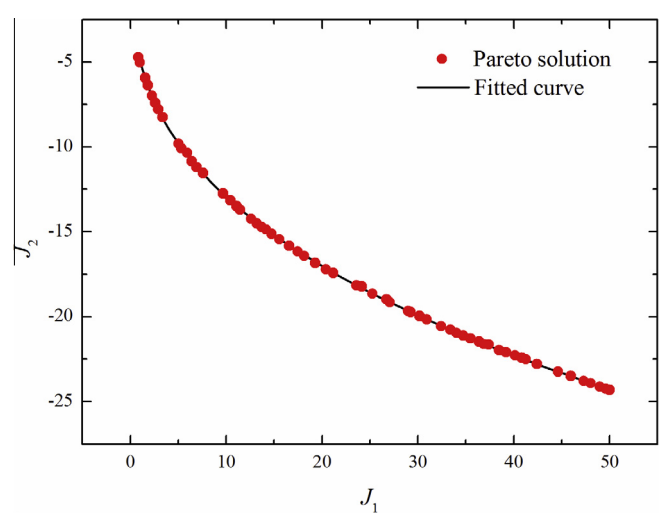

Fig. 6. Pareto solutions and fitted curve for $f < 50$.

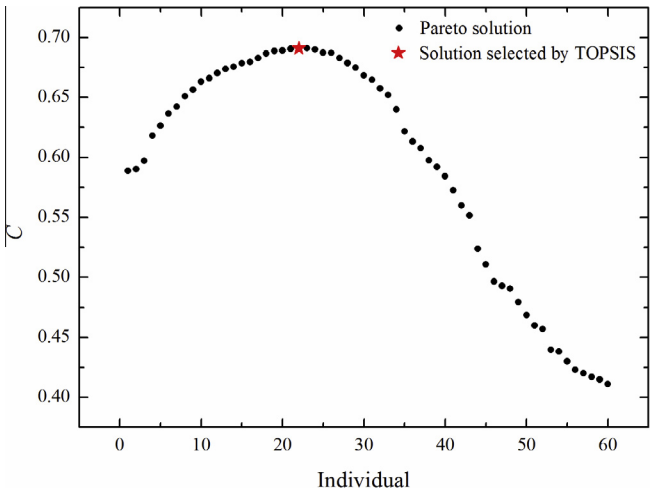

Fig. 7. Relative closeness to the ideal solution.

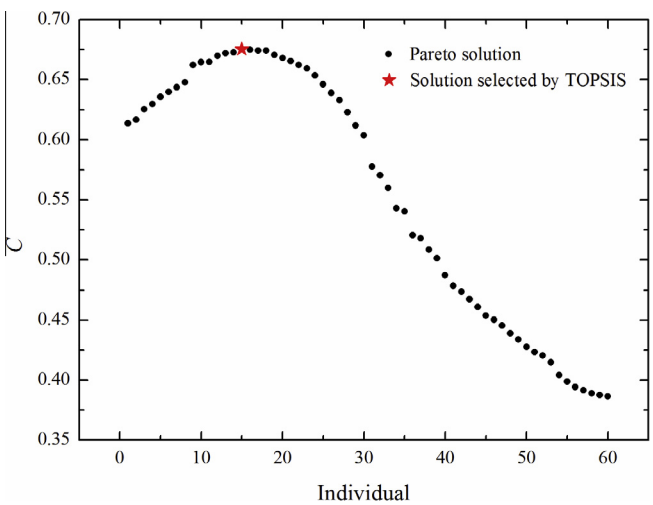

Fig. 8. Relative closeness to the ideal solution for $f < 50$.

$$y(x) = -5.925x^{0.3706} + 0.9729 \tag{26}$$

Comparing two individuals with the highest heat transfer coefficient in Figs. 5 and 6, it is found that Nu changes from 95.36 to 24.30 and f changes from 1729.65 to 49.99, respectively. It is noticed that all the values of J_1 are in the interval 0–50, which means the method of adding penalty function is valid for imposing constraints in present work.

The TOPSIS technique is subsequently employed to determine which solution has the best overall performance. In present study, the weighting matrix $(w)_j$ is [0.5 0.5]. The relative closeness to the ideal solution of alternatives is shown in Figs. 7 and 8. Results show that C varies from 0.411 to 0.691 without the penalty function and varies from 0.386 to 0.676 with the penalty function, respectively. Near the ends of Pareto front, individuals are generally far away from the positive ideal point. After ranking all individuals, the 22th solution in case 1 and the 15th solution in case 2 are respectively selected by TOPSIS technique. The optimized variables and performances are listed in Table. 2.

Fig. 9 shows the local Nusselt number varies along the whole tube for different conditions. It is noticed that the heat transfer performance is also improved at the entrance section and the exit section since porous ring changes the flow structure. After entering the porous section, Nusselt number increases significantly due to the porous ring. Besides, it is found that both porous rings have a fast effect on performance and more than 90% of the porous section is working in best condition. The maximum of local Nusselt number is 52.10 for the case 1 and 13.09 for the case 2, respectively.

Next, the optimal solutions for different situations are compared in Fig. 10. Nu_{max} represents the alternative which has the maximum Nusselt number in the Fig. 5. Compared with the alternative Nu_{max}, the optimal solution determined by TOPSIS drops 48.35% in Nusselt number while drops 82.21% in friction factor, respectively. It is obvious that TOPSIS is an effective method to balance two conflicting objectives. When we add the constraint $f < 50$ and make the further selection, it is found that the friction factor drops 99.43% while the Nusselt number drops 86.64%. This result indicates that the comprehensive performance may decrease after

Table 2
Optimized results under different conditions.

	R_1	R_2	ε	Da	f	$Nu_{average}$
Case 1: No penalty function	0.0538	0.894	0.824	3.41×10^{-8}	303.30	49.25
Case 2: With penalty function	0.0947	0.608	0.912	1.77×10^{-5}	9.67	12.74

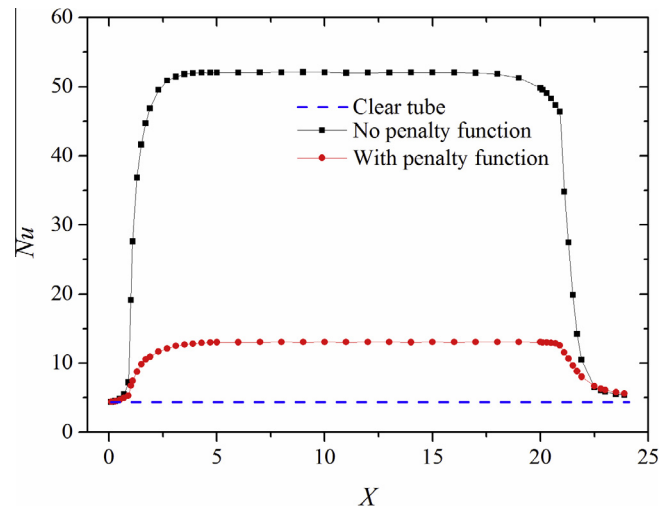

Fig. 9. Local Nusselt number distribution along the tube.

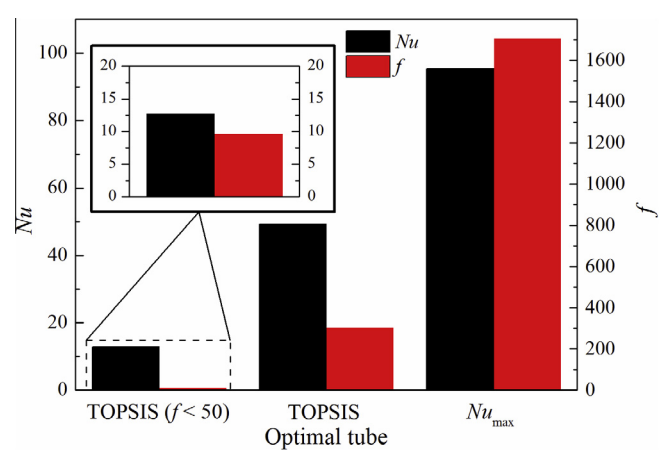

Fig. 10. Performances of optimal tubes under different situations.

adding the constraint in the objective function. However, this method is practical for making decision in the application when the resource such as pump power is limited.

5. Conclusion

In this paper, the configurations of porous media inserted in a tube have been optimized. The minimum *f* and the maximum *Nu* of the tube are two conflicting objectives simultaneously considered. In the optimization process, multi-objective genetic algorithm and CFD are coupled to solve the problem above and obtain a series of Pareto solutions. It is obvious from Pareto front that *f* significantly increases as *Nu* increases. Then, TOPSIS technique is applied to determine the best solution from the Pareto front. Results show that the solution determined by TOPSIS drops 48.35% in *Nu* while drops 82.21% in *f* in comparison with the alternative which has the maximum Nusselt number. Subsequently, we apply the penalty function instead of adding or modifying governing equations to restrain the flow resistance. It is proved that this method is effective without convergence difficulties and practical for utilizing limited resources.

Conflict of interest

None

Acknowledgment

The work is supported by the National Key Basic Research Program of China (973 Program) (2013CB228302) and the National Natural Science Foundation of China (51376069).

References

[1] N.B. Zheng, W. Liu, Z.C. Liu, P. Liu, F. Shan, A numerical study on heat transfer enhancement and the flow structure in a heat exchanger tube with discrete double inclined ribs, Appl. Therm. Eng. 90 (2015) 232–241.
[2] J.B. Wang, Z.C. Liu, F. Yuan, W. Liu, G. Chen, Convective heat transfer optimization in a circular tube based on local exergy destruction minimization, Int. J. Heat Mass Transfer 90 (2015) 49–57.
[3] J. Guo, Y.X. Yan, W. Liu, F.M. Jiang, A.W. Fan, Effects of upwind area of tube inserts on heat transfer and flow resistance characteristics of turbulent flow, Exp. Thermal Fluid Sci. 48 (2013) 147–155.
[4] B.I. Pavel, A.A. Mohamad, An experimental and numerical study on heat transfer enhancement for gas heat exchangers fitted with porous media, Int. J. Heat Mass Transfer 47 (23) (2004) 4939–4952.
[5] Z.F. Huang, A. Nakayama, K. Yang, C. Yang, W. Liu, Enhancing heat transfer in the core flow by using porous medium insert in a tube, Int. J. Heat Mass Transfer 53 (5–6) (2010) 1164–1174.
[6] R.L. Webb, Performance evaluation criteria for use of enhanced heat transfer surfaces in heat exchanger design, Int. J. Heat Mass Transfer 24 (4) (1981) 715–726.
[7] Z.J. Zheng, M.J. Li, Y.L. He, Optimization of porous insert configurations for heat transfer enhancement in tubes based on genetic algorithm and CFD, Int. J. Heat Mass Transfer 87 (2015) 376–379.
[8] J.Y. Yun, K.S. Lee, Influence of design parameters on the heat transfer and flow friction characteristics of the heat exchanger with slit fins, Int. J. Heat Mass Transfer 43 (14) (2000) 2529–2539.
[9] W. Liu, Z.C. Liu, L. Ma, Application of a multi-field synergy principle in the performance evaluation of convective heat transfer enhancement in a tube, Chin. Sci. Bull. 57 (13) (2012) 1600–1607.
[10] R. Long, B.D. Li, Z.C. Liu, W. Liu, Multi-objective optimization of a continuous thermally regenerative electrochemical cycle for waste heat recovery, , 93, Energy 93 (2015) 1022–1029. Part 1.
[11] A. Ahmadi, H. Moghimi, A.E. Nezhad, V.G. Agelidis, A.M. Sharaf, Multi-objective economic emission dispatch considering combined heat and power by normal boundary intersection method, Electric Power Syst Res 129 (2015) 32–43.
[12] K. Deb, S. Agrawal, A. Pratab, T. Meyarivan, A fast elitist non-dominated sorting genetic algorithm for multi-objective optimization: NSGA-II, in: Proceedings of the Parallel Problem Solving from Nature VI Conference, Springer. Lecture Notes in Computer Science No. 1917, Paris, France, 2000, pp. 849–858.
[13] Y. Ge, Z.C. Liu, W. Liu, G. Chen, Active optimization design theory and method for heat transfer unit and its application on shape design of cylinder in convective heat transfer, Int. J. Heat Mass Transfer 90 (2015) 702–709.
[14] C.L. Hwang, K. Yoon, Multiple Attribute Decision Making: Methods and Applications, Springer, Boca Raton, Florida, US, 1981.
[15] A.A. Mohamad, Heat transfer enhancements in heat exchangers fitted with porous media Part I: constant wall temperature, Int. J. Therm. Sci. 42 (4) (2003) 385–395.
[16] S. Ergun, Fluid flow through packed columns, Chem. Eng. Prog. 48 (1952) 89–94.
[17] M. Kaviany, Principles of Heat Transfer in Porous Media, Springer, New York, 1995.
[18] MathWorks Incorporated, User's Guide, MathWorks Incorporated Natick, 2010.
[19] J.Y. Jang, J.L. Chen, Forced convection in a parallel plate channel partially filled with a high porosity medium, Int. Commun. Heat Mass Transfer 19 (2) (1992) 263–273.
[20] N. Rudraiah, Forced convection in a parallel plate channel partially filled with a porous material, ASME J. Heat Transfer 107 (1985) 331–332.
[21] S. Sivanandam, S. Deepa, Introduction to Genetic Algorithms, Springer, Berlin, 2007.